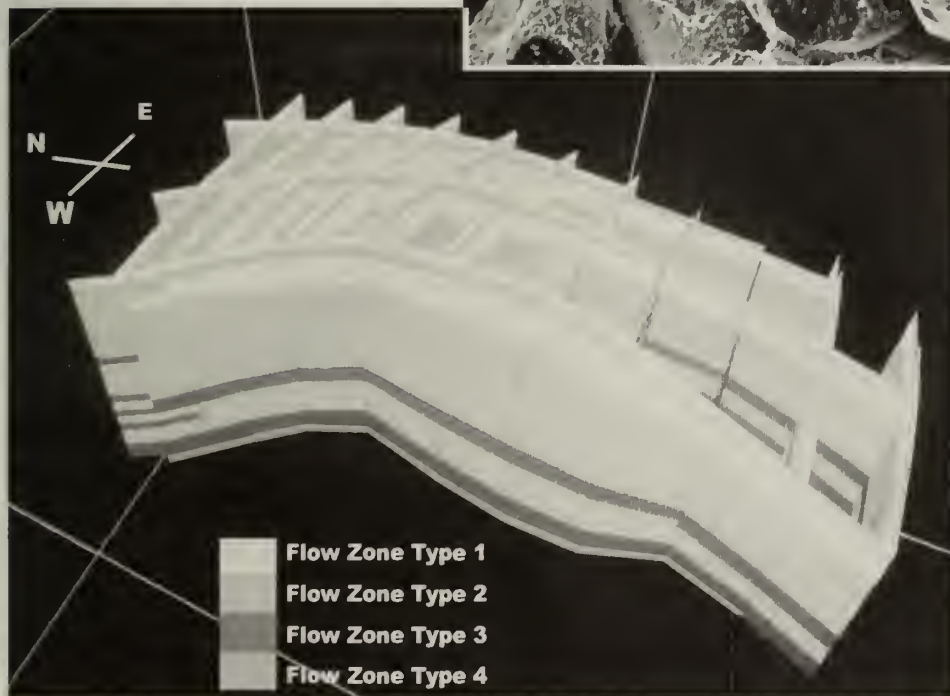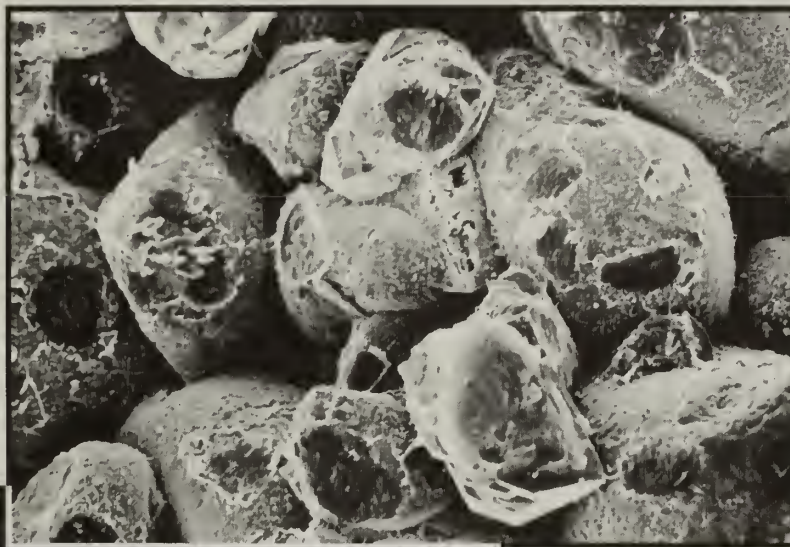Geol Survey

Integrated Geological and Engineering Study and Reservoir Simulation of the St. Peter Sandstone Gas Storage Reservoir at the Hillsboro Field, Montgomery County, Illinois

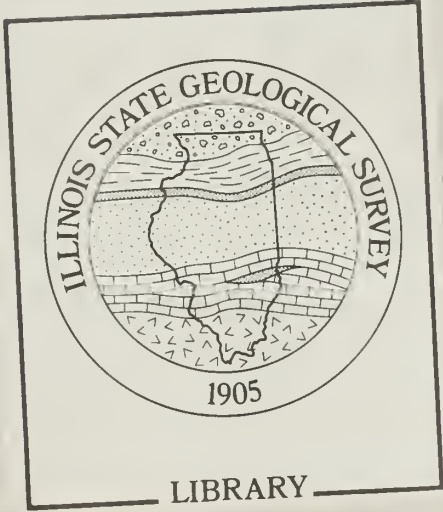Emmanuel O. Udegbunam, Bryan G. Huff, Curt Kemppainen, and Jim Morgan

Flow Zone Type 1
Flow Zone Type 2
Flow Zone Type 3
Flow Zone Type 4

Integrated Geological and Engineering Study and Reservoir Simulation of the St. Peter Sandstone Gas Storage Reservoir at the Hillsboro Field, Montgomery County, Illinois

Emmanuel O. Udegbunam and Bryan G. Huff
Illinois State Geological Survey, Champaign, Illinois

Curt Kemppainen and Jim Morgan
Illinois Power Company, Decatur, Illinois

DISCLAIMER

This report was prepared by the Illinois State Geological Survey (ISGS) as part of a cooperative project sponsored by the State of Illinois and the Illinois Power Company.

It presents reasonable interpretations of available scientific data. Any opinions, findings, conclusions, or recommendations expressed herein are those of the authors. Neither the ISGS, any individual members of the ISGS staff, the Illinois Department of Natural Resources, nor the Illinois Power Company assumes any liability with respect to the use of any information contained in this report. Trade names cited in this report are provided solely for the purpose of informing the public. Use of a particular product does not constitute an endorsement by the ISGS or the Illinois Power Company.

ACKNOWLEDGMENTS

CONTENTS

PLATES

TABLES

EXECUTIVE SUMMARY

Gas storage allows a reliable gas supply during the coldest weather season when transcontinental pipelines cannot supply enough gas to meet demand. Underground geologic structures, usually anticlines or domes, are located and tested for suitability as a gas storage reservoir, and when such a structure and reservoir is identified, wells are drilled into the storage material, generally a porous sandstone. Observation wells are drilled on the periphery and above the structure to monitor gas and water migration and detect possible leakage. During the summer, gas is pipelined in from remote areas and injected into the reservoir. This stored gas is used to augment normal pipeline supplies to meet winter heating demand.

ISGS researchers created a dynamic computer model of the Hillsboro gas storage project to simulate the behavior of gas and water within the St. Peter Sandstone reservoir at depths of approximately 3,200 feet. Hillsboro Field was chosen because of the availability of well records, the amount of drill core available for study, and available proprietary information from the field's owner, Illinois Power Company. The project simulated field-scale storage strategies to determine the maximum amount of gas that could be stored and withdrawn under scenarios of no further development, of adding wells, and of injection of gas into different horizons. The effects of these differences on gas deliverability were also simulated.

To construct the model, porosity and permeability values from drill core analyses were correlated with geophysical logs so that these values could be calculated for wells without core. The porosity and permeability values were then used to calculate flow zone indices and to correlate flow zones of similar character within the reservoir. All of these values were entered into a geocellular model that could dynamically and simultaneously evaluate all these parameters and calculate changing fluid saturations and two-phase flow. Differences in reservoir quality noted on geophysical logs were petrographically analyzed for wells with core. Four types of porosity, caused by differences in sorting and grain size, were observed. They are believed to be the major influence on the delineation and continuity of the flow zones calculated by this model.

After construction, the model was tested and calibrated using historical injection and production data. When reservoir performance satisfactorily matched historical values, several different injection/withdrawal strategies were modeled to predict reservoir behavior. It was found that with no further development total gas inventory could be expanded from 21.7 to 23.8 billion standard cubic feet (BSCF) without spill point leakage. A maximum peak withdrawal of 150 million cubic feet of gas per day (MMCFGD) could be achieved as long as no more than 80% of the working gas was withdrawn. The peak-day rate fell to 125 MMCFGD when 85% or more of the working gas was produced prior to the peak day. Gas injection into lower horizons resulted in gas movement into the upper horizon because of vertical transmissibility. Inventory increased to 30 BSCF. The peak withdrawal of 125 MMCFGD could not be achieved if the upper layer was not open for production. A combination of injection into the lower layers and production from the upper layers allowed a peak withdrawal of 147.7 MMCFGD with up to 93% of the working gas produced. Addition of new wells gave an incremental increase in gas deliverability of 11 MMCFGD per well and a total additional gas withdrawal of 0.17 BSCF.

ABSTRACT

This report is a synthesis of two major studies that investigated the geology of the Hillsboro Gas Storage Field, characterized the St. Peter Sandstone (Ordovician) reservoir, and incorporated this information in an integrated computerized reservoir

model for reservoir simulation and storage management (Udegbunam and Huff 1994, Udegbunam et al. 1995). Petrophysical analyses revealed four distinct flow units in six cored wells. These flow units correspond to four lithologies identified by thin-section petrography. Three-dimensional (3-D), field-wide visualizations of distributions of petrophysically derived flow units show considerable vertical variability but lateral continuity. This finding explains why it has been easier to develop the gas storage bubble within the reservoir laterally than vertically.

A 3-D reservoir model developed from stratigraphic and petrophysical data was used to understand the past behavior of the Hillsboro Gas Storage Field and to investigate the field's performance under various development scenarios. Twenty-two years of gas storage reservoir history, including the initial gas bubble development and seasonal gas injection and production cycles, were examined with a full-field, gas-water, reservoir simulation model. After the simulations were sucessfully matched with historical gas storage performce, investigators examined the key questions of determining the maximum possible total gas-in-place volume without gas loss and the optimum base load volume that permits the achievement of the peak-day rate requirements.

The results from various simulated development strategies suggested that the gas-water front is already in the vicinity of the west observation well and that increasing the field's total gas-in-place volume would cause gas to migrate beyond the east, north, and west observation wells. The results also suggested that storage enlargement through gas injection into the lower layers may not prevent gas migration. Simulated gas deliverability results suggested that a peak-day rate of about 150 MMSCFD could be achieved with up to 80% of the working gas produced before the peak day. They also showed that the peak-day rate would fall below 125 MMSCFD when 85% or more of the working gas was produced before the peak day. Furthermore, the simulated results suggested that the addition of strategically located new wells could boost the gas deliverability.

INTRODUCTION

The Hillsboro Gas Storage Field project, which began in August 1973, underlies more than 4,000 surface acres (16.2 km²). It contained a total natural gas inventory of 21.7 BCF (614.5×10^3 m³) at the start of the 1994 withdrawal season. The estimate of working gas inventory, the amount that can be injected and withdrawn each season, is 7.6 BCF (212.4×10^3 m³) or 35% of the total gas in storage.

Owned and operated by Illinois Power Company, the Hillsboro Field consists of an anticlinal dome located in Sections 28, 29, and 31–34, 10N-3W and Sections 4, 5, 8,and 9, 9N-3W in Montgomery County, Illinois, and a storage reservoir in the St. Peter Sandstone (Ordovician) (figs. 1 and 2). The crest of the field lies at an elevation of –2,490 feet (–759 m) below sea level. Fourteen gas wells, four water (observation) wells, and four shallow wells provided the well control and data for both the geologic modeling and interpretation and the reservoir simulation modeling (Udegbunam and Huff 1994, Udegbunam et al. 1995). The primary objectives of this study include the following:

- investigate the geology of the Hillsboro Gas Storage Field: its structure, lithological and petrographical variations, internal stratigraphy, flow zones, and flow barriers;

- characterize the St. Peter Sandstone reservoir at Hillsboro Gas Storage Field;

- generate a 3-D geologic model of the field;

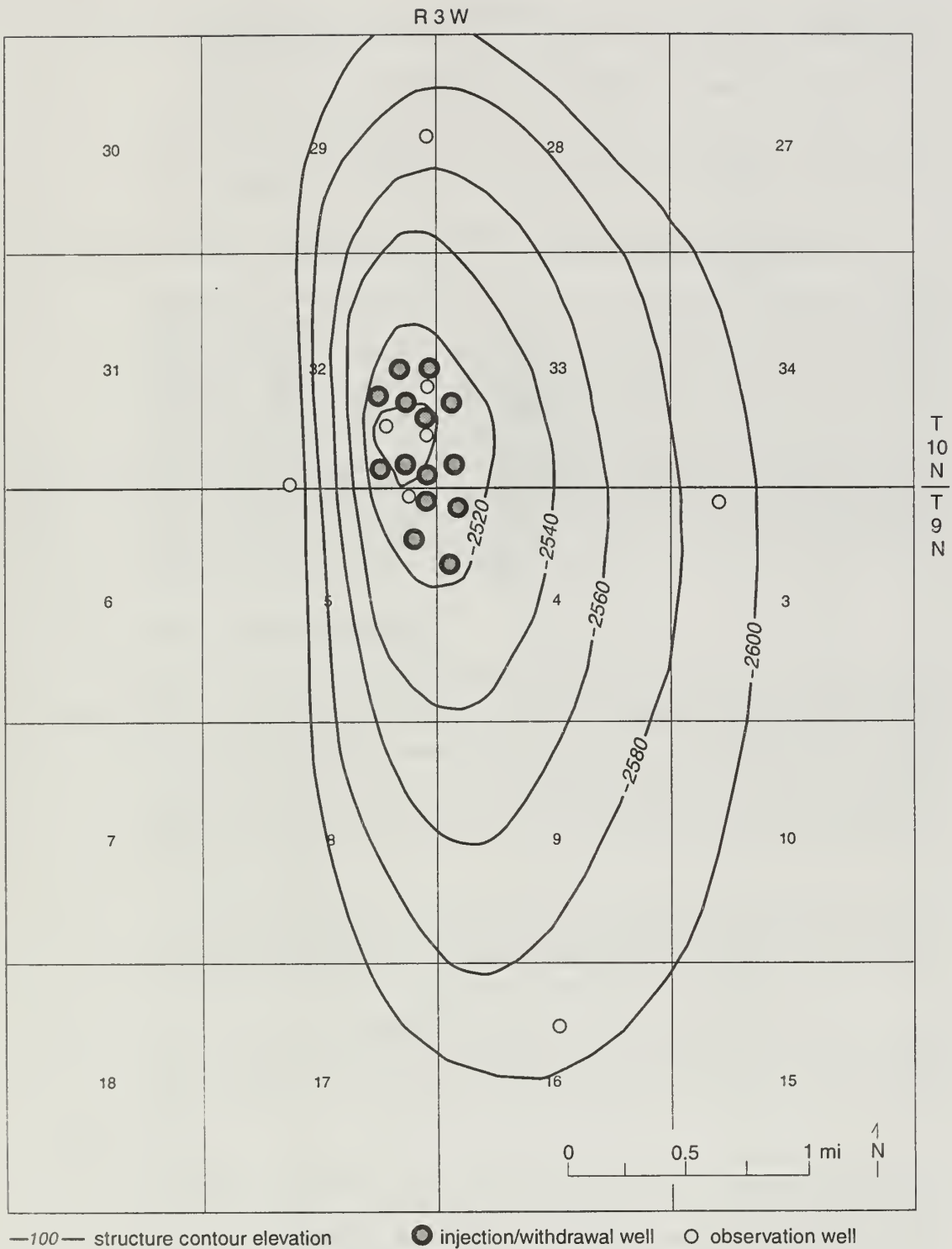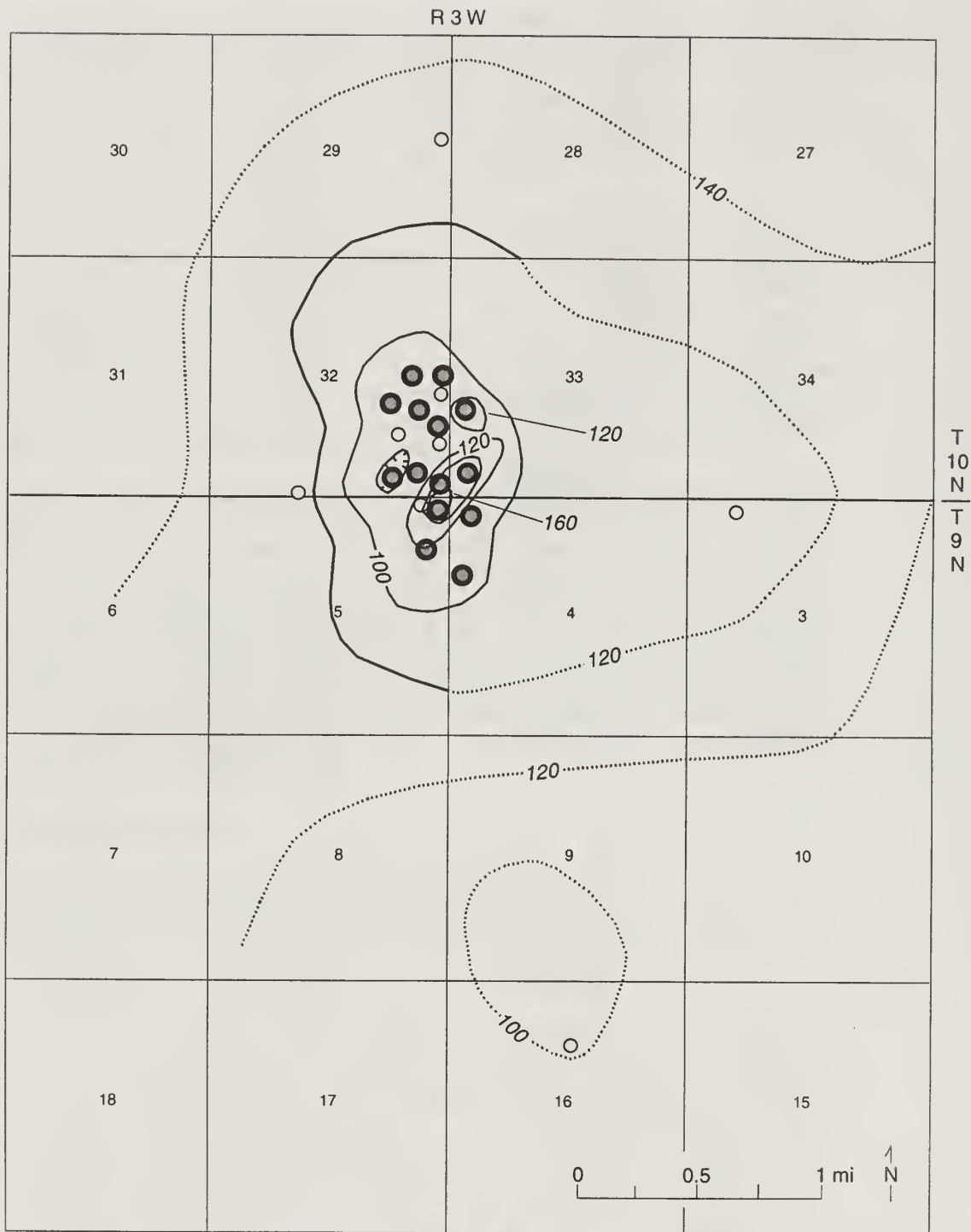- upscale the 3-D geologic model into a 3-D fluid flow model;

Figure 1 Structure of the top of the St. Peter Sandstone in the Hillsboro area. Contour interval = 20 feet.

Figure 2 Isopach of the St. Peter Sandstone at the Hillsboro Field. Contour interval = 20 feet.

- perform numerical simulation of the development and operation of the Hillsboro Field;

- match simulated gas-in-place inventory, observation well pressures, and gas thicknesses to the historical data;

- predict the maximum gas inventory possible in the Hillsboro Field without gas loss or gas encroachment on the water wells; and

- determine the optimum base load that permits the achievement of the peak-day rate requirement at various strategies of field development.

Interpretation of the depositional environments of the St. Peter Sandstone is not part of this study but has been reported by other workers (Dapples 1955, Dott et al. 1986, Shaw and Schreiber 1991, Fu et al. 1994). Dapples (1955) stated that the St. Peter Sandstone was deposited in a series of coalescent shoreline sands produced by a generally northward transgression over a stable shelf. Dott et al. (1986) expanded on this by recognizing the St. Peter as the product of aeolian sands that accumulated on top of an unconformity and that were subsequently reworked by marine transgression. Shaw and Schreiber (1991), examining a core from Hillsboro Field, recognized deposits from nearshore subtidal sandstone environments as well those from biogenically reworked foreshore, shallow subtidal, high-energy deposits. Fu et al. (1994) briefly synthesized the latter two interpretations.

FIELD DEVELOPMENT

To date, 14 injection/withdrawal wells have been completed in the St. Peter Sandstone. One of the gas wells, the Truitt no. 1, was being used for monitoring the gas bubble pressure. Eight wells monitor water level in the field. Four of these wells, the House no. 1, Gregg no. 1, Lipe no. 1, and King no. 1, were completed in the St. Peter Sandstone to observe pressure changes in the aquifer surrounding the connected gas bubble (table 1). The other four were used to monitor the caprock and other shallower formations. All Hillsboro wells were completed with 5.5-inch or 7-inch casing and perforated at 8 to 12 shots per foot.

Water encroachment resulted in watering-out of some perimeter gas wells. A small amount of water was produced, and, on average, about 260 barrels of water were collected in the well separators for every 7.6 BCF of gas withdrawn annually. Produced water was sent via flowlines to a central tank and then to a disposal well.

Changes in gas zone thickness were primarily monitored at the wells. Neutron logs were run once in the spring and once in the fall. Gas thicknesses were used in this model to verify saturation matches because data were not available for the produced gas-water ratio.

The peak-day rate in the field with the present well configuration has been limited to 125 MMSCFD because of sand production during gas withdrawal. Hillsboro wells have had a history of sand production. Three wells, the Truitt no. 2, Morrell no. 2, and IP no.1, have sanded up and been treated with resin. Two other wells, the Greenwood no. 2 and IP no. 4, sanded up during the 1994–95 withdrawal season and have been scheduled for similar treatment. It is hoped that with treatment the peak-day rate can reach 150 MMSCFD and not have sand produced.

Subsurface Geology

Stratigraphy   In this area, the St. Peter Sandstone ranges between 93 and 166 feet thick (fig. 2) because of deposition on the irregular karst surface of the underlying

Table 1 Well names and corresponding simulation model numbers

Well names	Well number in the reservoir simulation model	Type of well
Morrell no. 2	1	Gas I/W
Gregg no. 2	2	Gas I/W
Roth-Boyle no. 1	3	Gas I/W
Greenwood no. 1	4	Gas I/W
Truitt no. 2	5	Gas I/W
Morrell no.3	6	Gas I/W
Lipe no. 1	7	Water observation
Gregg no.1	8	Water observation
IP no. 2	9	Gas I/W
Greenwood no. 2	10	Gas I/W
IPC no. 1	11	Gas I/W
Snyder no. 1	12	Gas I/W
IP no. 3	13	Gas I/W
IP no. 4	14	Water observation
House no. 1	15	Water observation
Snyder no. 2	16	Gas I/W
Truitt no. 1	17	Gas observation
King no. 1	18	Water observation
IPC no. 5	19	Simulated new gas I/W
IPC no. 6	20	Simulated new gas I/W
IPC no. 7	21	Simulated new gas I/W

Shakopee Dolomite (Ordovician). The St. Peter Sandstone is overlain by the Joachim Dolomite (Ordovician), which provides the seal for the gas storage reservoir (fig. 3).

The thinning of the St. Peter Sandstone shown on the isopach map (fig. 2) is over a high on the Shakopee Dolomite, also located in the southeastern quarter of Section 32, and shows that this area has been topographically high since at least the early Ordovician. Thickened stratigraphic sections on the flanks of the structure were noted for the middle Ordovician, Devonian, lower Valmeyer, and Pennsylvanian sediments. The thickened strata indicate that uplift occurred during deposition of these units.

Log characteristics   Spontaneous potential and gamma ray curves through the St. Peter are relatively featureless with the exception of an increased gamma ray count approximately 3 feet below the top of the sandstone (fig. 3). Core shows this zone to be composed of fissile black shale. Another increase in gamma radiation is consistently observed approximately 100 feet into the section. Green shales are contained in core from this zone.

Neutron and density porosity logs are somewhat more definitive, showing porosity kicks of about 4% to 6%, which are persistent and can sometimes be traced several miles across the entire field. This continuity is attributed to sedimentological and biological reworking of a layer of sediments into a laterally homogenous deposit (T.H. Shaw, Exxon Corp, personal communication 1994). With deposition of new sediments, the process repeats itself, and a stacked series of laterally continuous layers is formed.
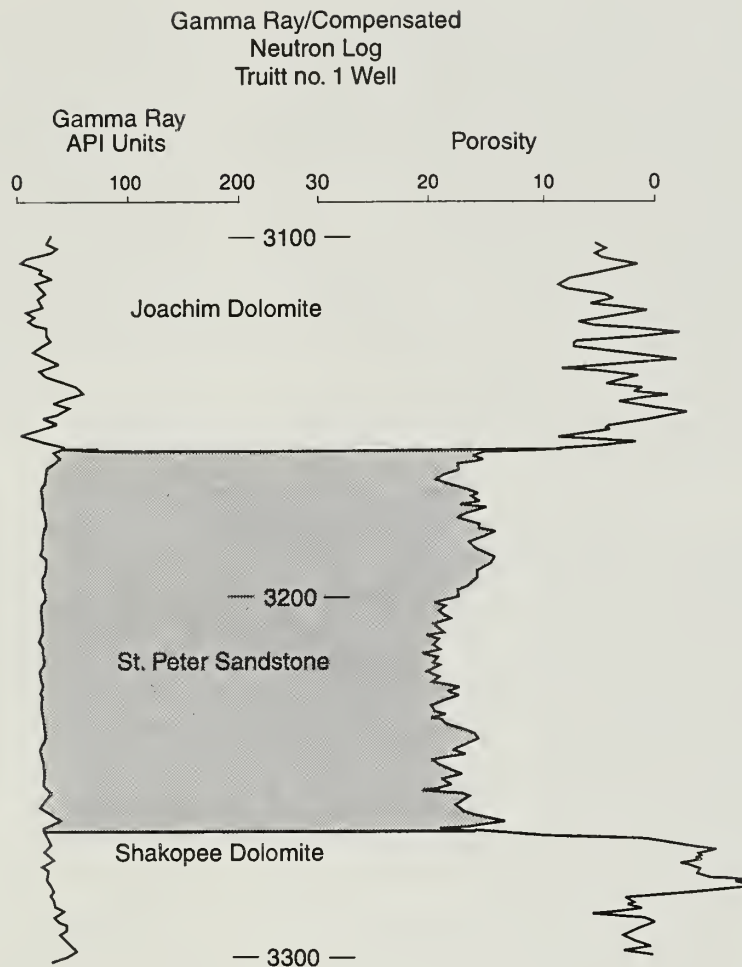
Figure 3 Gamma ray and density porosity log through the St. Peter Sandstone interval from the Truitt no. 1 well, Hillsboro Field, Section 4, 9N-3W Montgomery County, Illinois.

Petrography

Thirty samples of representative lithologies from the Truitt no. 1 and Morrell no. 2 wells were thin-sectioned and analyzed using a petrographic microscope (plate 1, a–d). Samples from these wells were also examined using a scanning electron microscope and x-ray dispersive chemical analysis (plate 1, e and f).

Framework grains Up to 99% of the rock is made up of well-rounded quartz grains. A few metaquartzite grains are also present. Other grains occurring in very small amounts are potassium feldspar, green hornblende, and zircon. Framework grains range in size from silt to coarse sand. Sorting ranges from very poor to excellent. Grains may be (1) poorly sorted and homogenously distributed; (2) continuous or discontinuous layers, well sorted, and homogenously distributed; or (3) any combination of these configurations within the area of a single thin section. Horizontal layers of fine-grained material are commonly observed and are believed to be the primary cause of low vertical permeabilities relative to horizontal permeabilities.
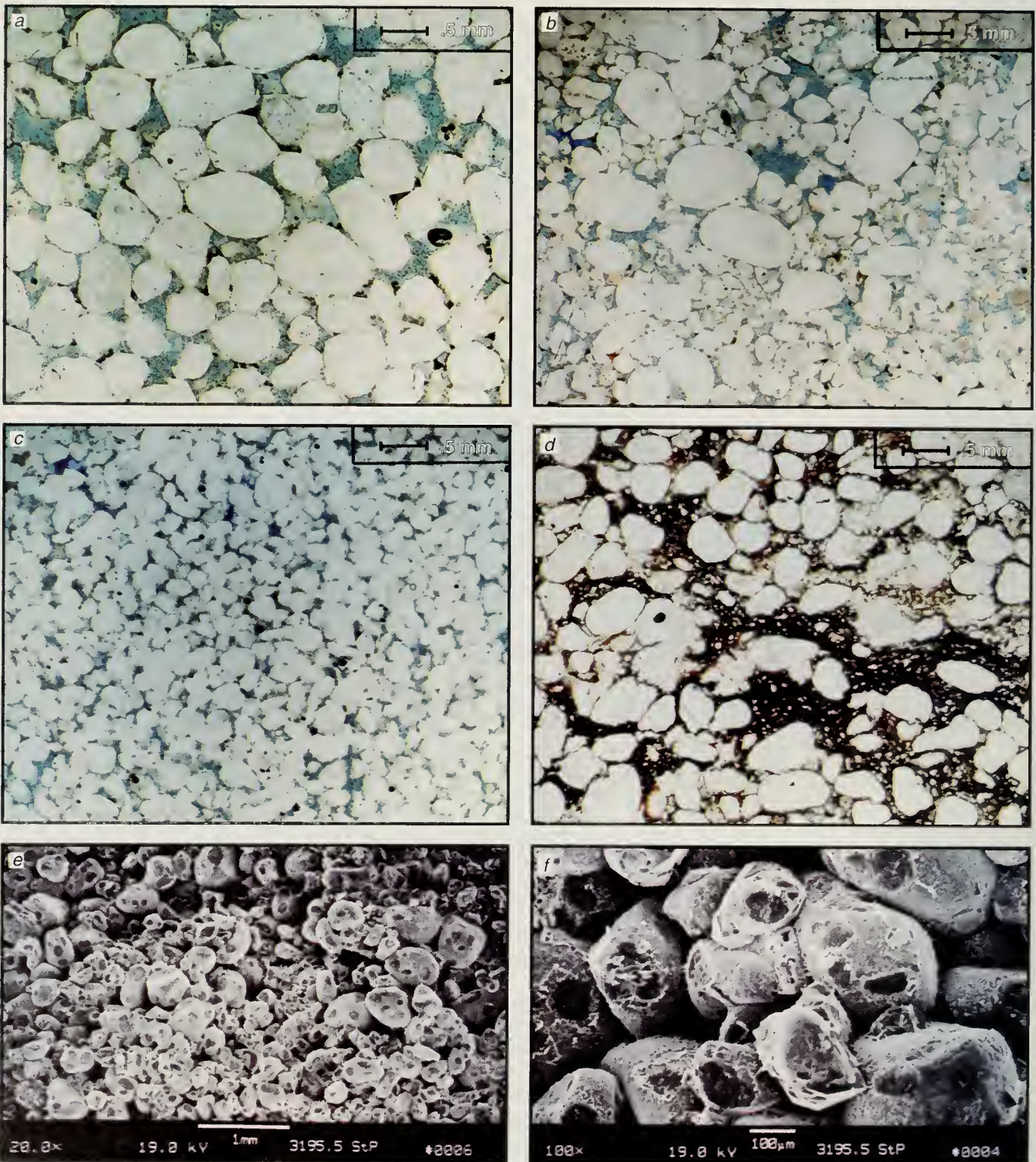
Plate 1 Photomicrographs of sandstone samples impregnated with blue epoxy to show porosity. (*a*) Sandstone type 1: Note large grains and pores, good sorting, and quartz overgrowths, Truitt no. 1 well, depth 3,162 feet, 25×, bar scale = 0.5 mm. (*b*) Sandstone type 2: Note poor sorting, mixed pore sizes, Morrell no. 2 well, depth 3,191 feet, 25×, bar scale = 0.5 mm. (*c*) Sandstone type 3: Note fine grain size, good sorting, and small pores, Truitt no. 1 well, depth 3,186 feet, 25×, bar scale = 0.5 mm. (*d*) Sandstone type 4: Note poor sorting, lack of porosity, algal kerogen (dark diagonal band), and calcite cement. Compactional features visible include concavo-convex grain contacts and styolitic, sutured contacts, Truitt no. 1 well, depth 3,160 feet, 25×, bar scale = 0.5 mm. Scanning electron microscope images of the St. Peter Sandstone from the Hillsboro Gas Storage Field. (*e*) Typical reservoir sand showing mixed grain sizes and abundant porosity, Truitt no. 1 well, depth 3,195.5 feet, 20×. (*f*) Close-up of sandstone shown in *e* showing clay coatings, scattered quartz overgrowths, and rare feldspar (etched rhombohedron in center of image), Truitt no. 1 well, depth 3,195.5 feet, 100×.

Cements and other pore-occluding materials Cements, in order of their precipitation, are dust rims consisting of illite and micrometer-size potassium feldspar and quartz overgrowths, interstitial calcite, and chalcedony. Very minor amounts of intergranular potassium feldspar of indeterminate timing have also precipitated and now show dissolution features. The dust rims are on virtually every grain but do not substantially reduce pore volume (plate 1, *e* and *f*). Quartz overgrowths are common, but range from poorly to extremely well-developed. Where well-developed, they occlude significant pore volumes and constrict pore throats. In zones with substantial quartz overgrowths, pore throats are approximately 100 μm wide, and the rock is still a viable reservoir. Calcite occurs sporadically in small zones, generally a few millimeters to 1 cm in area. Calcite was observed throughout the St. Peter Formation but is more common in the upper part. Where calcite is present, pores are totally blocked except at boundary pores where the calcite crystals terminate. Chalcedony is a very rare cement and was observed to fill only one pore in one thin section.

Lithological Definitions of the St. Peter Sandstone

Whole core inspections and the petrographic interpretations show that there are four sandstone porosity types in the St. Peter Sandstone at the Hillsboro Gas Storage Field. Fu et al. (1994) independently confirmed these four porosity types in their study.

Sandstone type 1 consists of coarse-grained, well-sorted sandstone with well-developed quartz overgrowths and large, open pores (plate 1, *a*). Although quartz overgrowths are well developed, porosity and permeability are high.

Sandstone type 2, the most common type of rock observed, consists of moderately to poorly sorted, coarse- and fine-grained sandstone with large and small pores (plate 1, *b*). Development of quartz overgrowths is variable. Porosity and permeability are reduced, as compared with sandstone type 1, primarily by smaller grains blocking larger pores and reducing average pore throat size. Variations of this lithology caused by differences in the relative abundance of fine and coarse grains, size segregation in layers, and cement development create a wide, gradational range of porosity and permeability values.

Sandstone type 3 consists of well-sorted, fine-grained sandstone with well-developed quartz overgrowths and large, open pores (plate 1, *c*). Although quartz overgrowths are well developed, porosity and permeability are high.

Sandstone type 4 consists of very poorly sorted sand, silt, and clay with calcite cement (plate 1, *d*). Porosity is generally poor but well-developed in some small areas. Permeability is poor because of lack of pore connectivity and small pore throats. Porosity and permeability have also been reduced by styolitic dissolution. This lithology is most commonly found in the uppermost St. Peter and as scattered occurrences in lower parts of the unit.

Petrophysical Analyses and Flow Units

Six of the 14 active wells were cored: Greenwood no.1, Morrell no. 2, House no. 1, King no. 1, Synder no. 2, and the Truitt no. 1. The semi-log plot of core permeability versus core porosity (fig. 4) shows considerable scatter, which indicates the presence of more than one petrophysical flow unit (Abbaszadeh et al. 1996). The flow unit concept was used in this work to separate the St. Peter Sandstone into flow zones, which are applied in building the model for reservoir simulation.
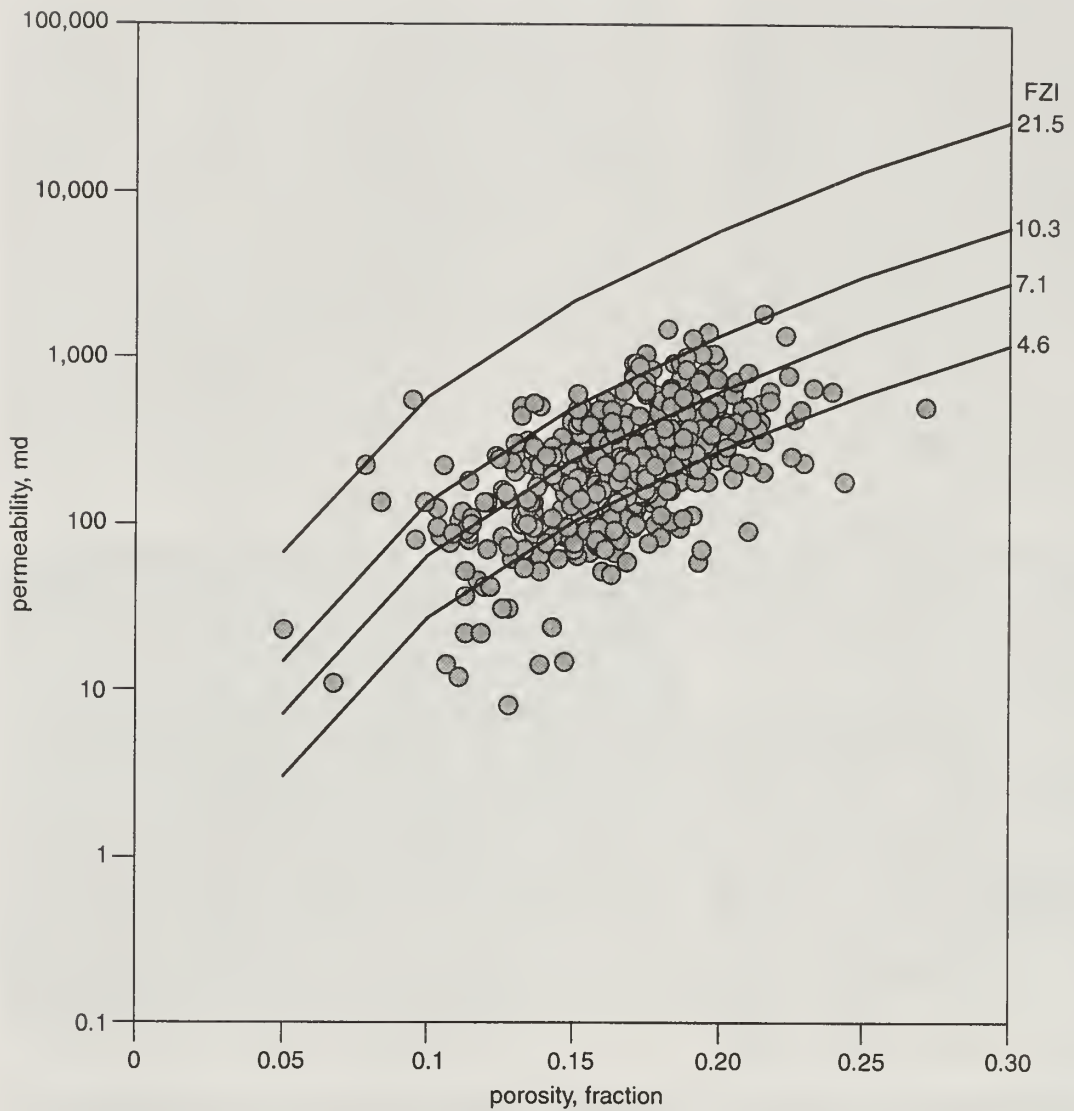
Figure 4 Permeability-porosity crossplot showing correlations for four major hydraulic units.

The flow unit concept defines the reservoir's homogeneous flow zones by the flow zone indicator (FZI) (Amaefule et al. 1993, Udegbunam and Huff 1994). The FZI, first defined by Amaefule et al. (1993) and further explained by Abbaszadeh et al. (1996), is determined from core-derived permeability (K) and porosity values (ϕ) and delineates reservoir intervals into hydraulic flow units based on the mean hydraulic radii of pore throats:

$$FZI = 0.0314\sqrt{(K/\phi)}\frac{(1-\phi)}{\phi} .$$
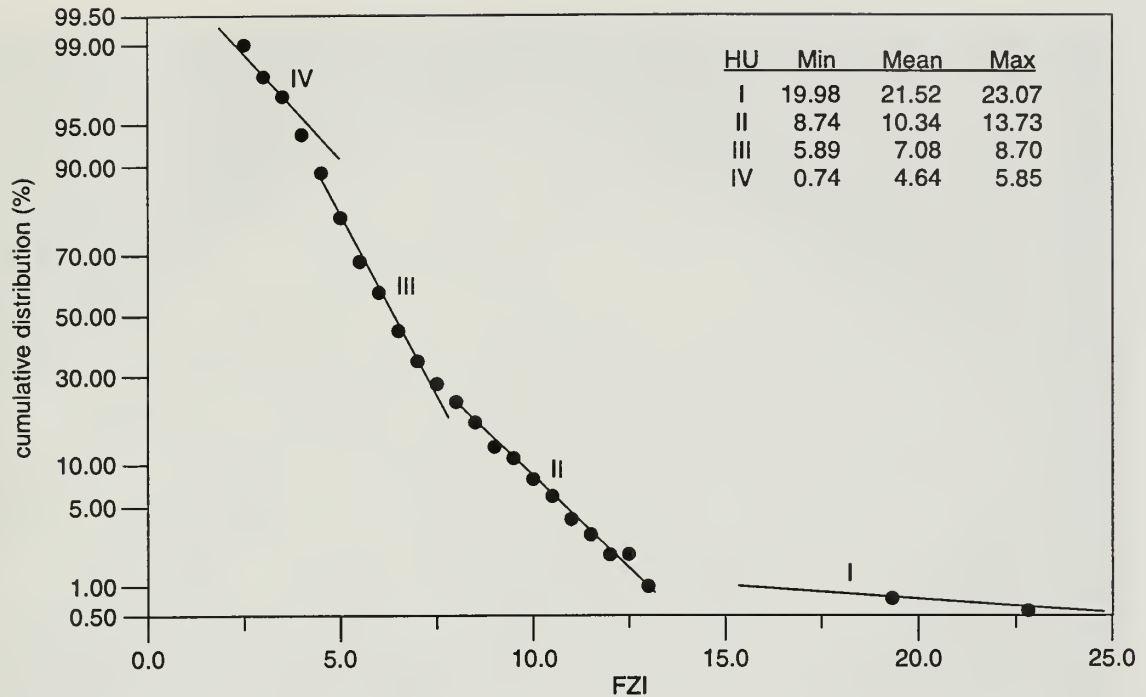
Figure 5 Probability plot of FZI data for the St. Peter Sandstone reservoir, Hillsboro Field. HU, hydraulic unit.

Reservoir Characterization Aided by Flow Units

Reservoir zonation The FZI values, determined from measured porosity and permeability, were used to divide the formation into flow units that control flow in the porous media. Each flow unit consists of a range of FZI values and a mean value that describes that FZI range. Amaefule et al. (1993) and Abbaszadeh et al. (1996) presented methods for hydraulic unit classification. A probability plot of the FZI typically shows straight line segments, the number of which depends on the number of flow units in the system. Each distinct straight line segment corresponds to a flow unit.

The probability plot of the FZI data shows that the St. Peter sandstone has four distinct flow units (fig. 5). The flow-unit classification was found by cluster analysis using the SYSTAT software (Wilkinson 1989). A fence diagram of the hydraulic units shows that the hydraulic units are more continuous laterally than they are vertically (fig. 6).

Initial and residual gas saturation Amaefule et al. (1993) showed that the initial (S_{gi}) and residual (S_{gr}) gas saturation in Land's theory (1968) can be related to FZI:

$$\frac{1}{S_{gr}} - \frac{1}{S_{gi}} = \frac{C}{S_{gmax}} = f(FZI)$$

where C = Land's constant, and S_{gmax} = maximum gas saturation. Table 2 is a summary of the relative permeabilities for gas and water of three St. Peter Sandstone core
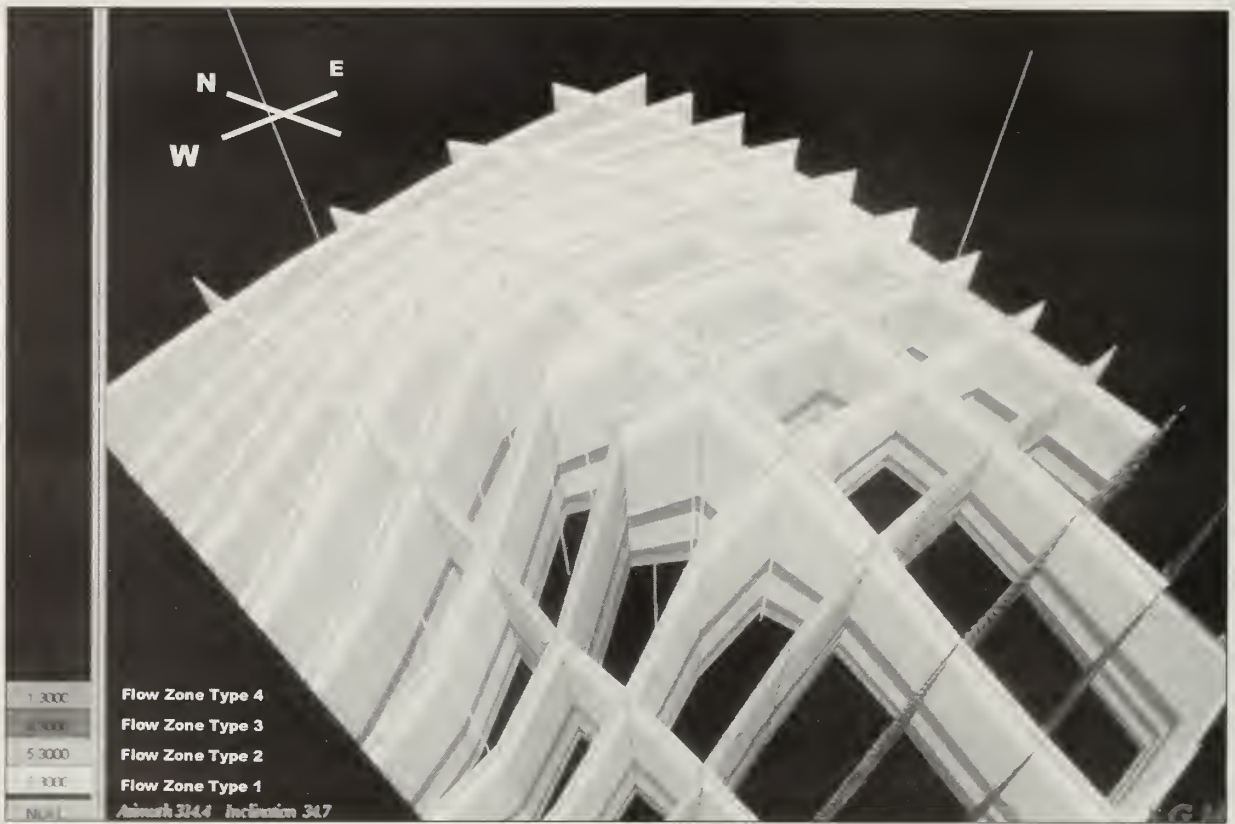
Figure 6 Fence diagram showing distribution of the hydraulic flow units of the St. Peter Sandstone reservoir, Hillsboro Field.

samples from the Hillsboro Gas Storage Field. A regression of the imbibition end-point gas saturations to FZI gives the following equation:

$$\frac{C}{S_{gmax}} = 0.2093e^{0.281\,FZI}.$$

The residual gas saturation corresponding to the initial gas saturation at the initial imbibition can be evaluated with this equation (fig. 7).

Geologic Modeling

The 3-D geologic models of the storage reservoir were created in this study with the help of the Stratigraphic Geocellular Modeling™ (SGM) software (Stratamodel Inc. 1993), which divides the gross reservoir volume into a large number of cells. A porosity model was constructed on the basis of the core-derived porosities, which ranged from 13% to 19.5%, with an average of 17%. Porosities in uncored wells were determined from the log-to-core porosity relationships. The horizontal and vertical core permeabilities range from 20 millidarcies (md) to more than 1,000 md. The unstressed, surface-derived values were utilized in the model because the St. Peter Sandstone at Hillsboro Field has excellent reservoir properties, and the effects of confining pressure on the reservoir quality were considered minimal. Permeabilities of uncored intervals were determined by attribute interpolation routines within the SGM.

Table 2 Initial and residual gas saturations from the core flood data on the St. Peter Sandstone samples

S_{gi}	S_{gr}	C/S_{gmax}	K (md)	ϕ	FZI
0.616	0.135	5.784031	1010	0.175	11.24572
0.676	0.192	3.729043	766	0.17	10.29079
0.650	0.256	2.367788	478	0.15	10.04444
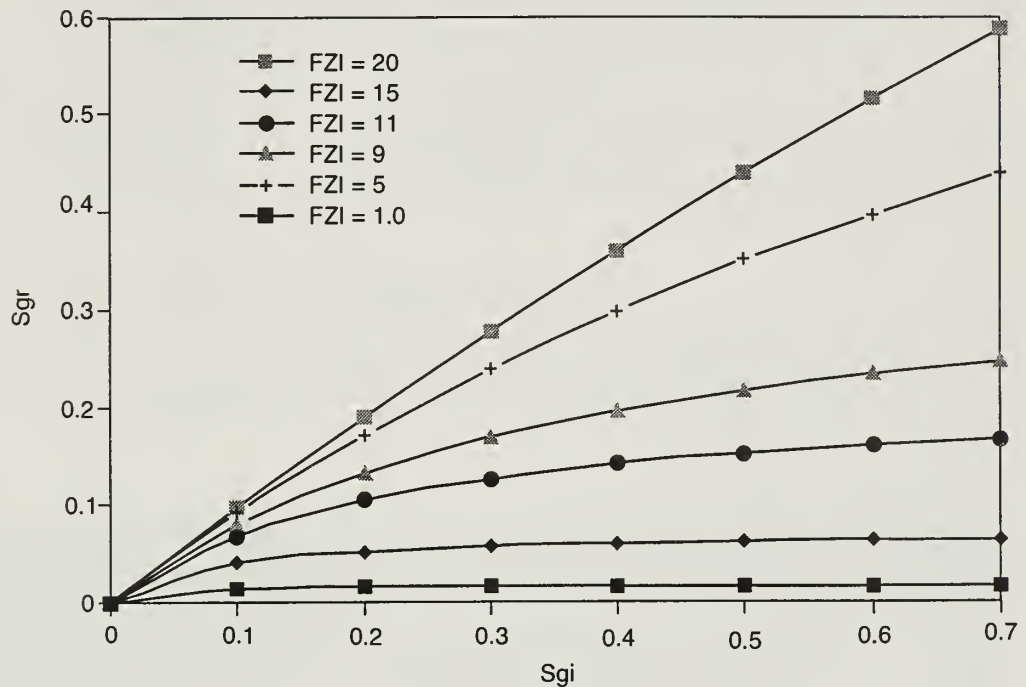
Figure 7 Cross-plots of initial and residual gas saturations at different FZI values.

Development of the Hillsboro Reservoir Flow Model

Reservoir simulation layers were created interactively with the aid of GeoLink™, a reservoir delineation software. The FZI values, derived from measured permeability and porosity values, provided the basis for visual and interactive delineation of the reservoir into simulation layers. A 20 × 28 grid overlay (fig. 8a) created with the Western Atlas Software's grid generator (GRIDGENR™) was used to produce a 20 × 28 × 3-cell, reservoir simulation flow model (fig 8b).

Initialization of the Hillsboro Reservoir Flow Model

The Western Atlas International (1994) VIP-CORE simulator was applied in this two-phase, gas-water, 3-D simulation model. Fluid and reservoir data necessary for initializing the reservoir model prior to the time-dependent simulations are described.

Porosity and permeability The porosity and permeability data needed to initialize the reservoir simulation model originated from the petrophysical model. The unique relationship between porosity and permeability within a given hydraulic flow unit was
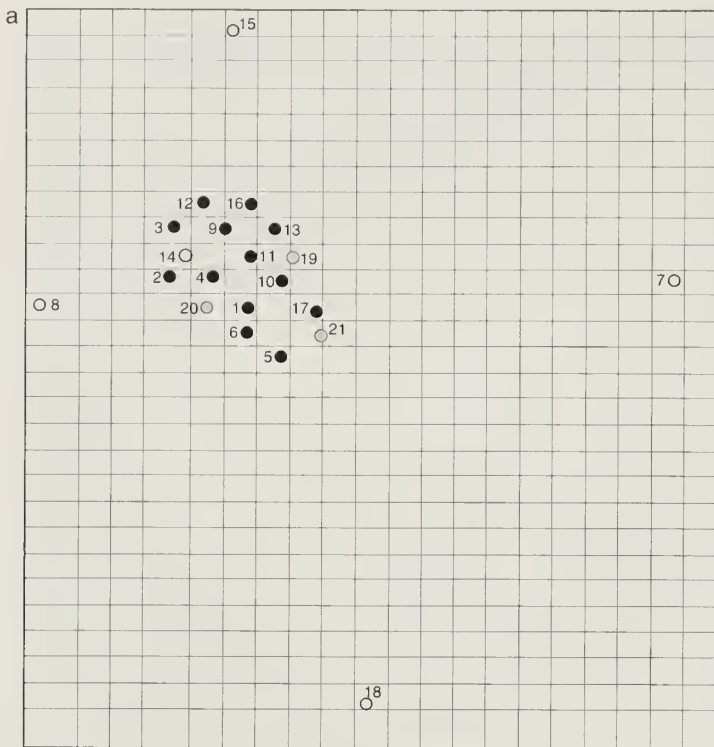
No.	WELL NAME
1	Morrell no. 2
2	Gregg no. 2
3	R. Boyle no. 1
4	Greenwood no. 1
5	Truitt no. 2
6	Morrell no. 3
7	Lipe no.1
8	Gregg no. 1
9	IP no. 2
10	Greenwood no. 2
11	IPC no. 1
12	Synder no. 1
13	IP no. 3
14	IP no. 4
15	House no. 1
16	Synder no. 2
17	Truitt no. 1
18	King no. 1
19	IP no. 5
20	IP no. 6
21	IP no. 7

● gas well
○ observation well
○ simulated well

Figure 8 Reservoir simulation grid (28 × 20) overlay (a) was used to produce the reservoir simulation flow model (b) of the St. Peter Sandstone. High water saturations are represented by light grays; high gas saturations are represented by dark grays.

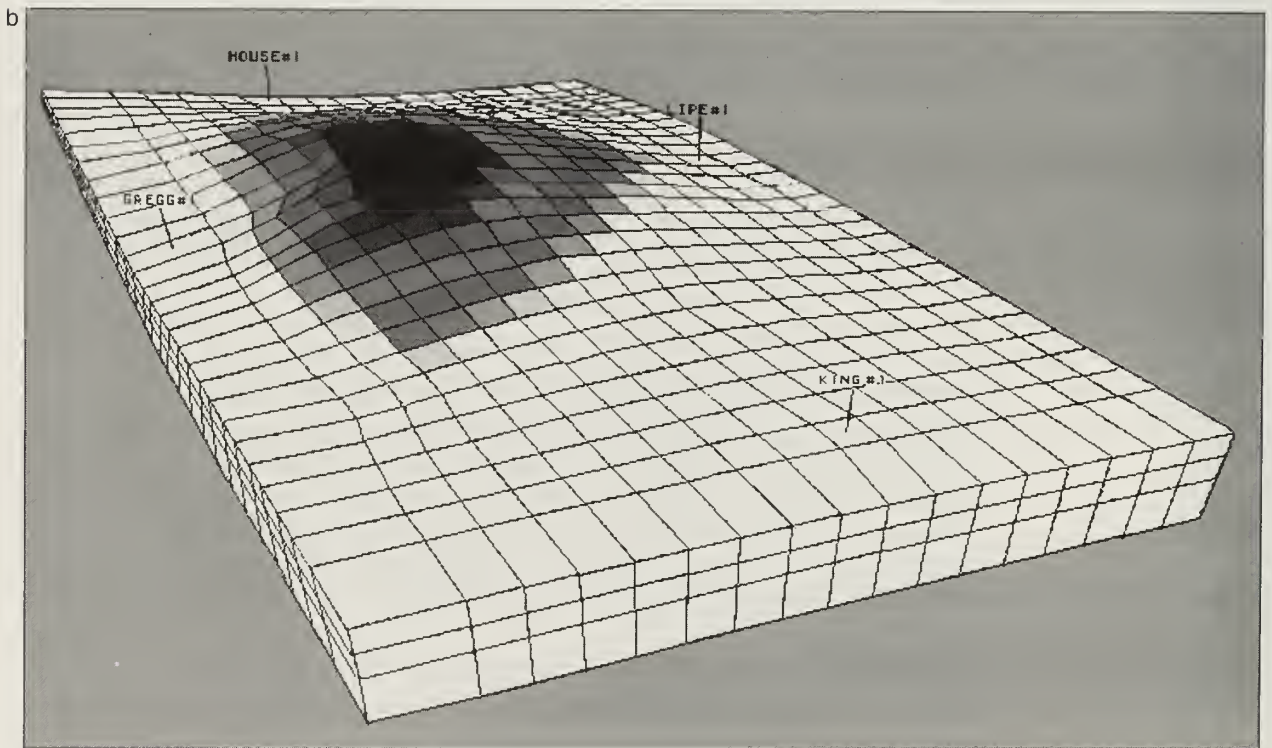used to estimate the permeability in uncored wells and in the interwell intervals. The values of permeability and porosity in each grid block were automatically interpolated during the grid generation process.

Relative permeability　The relative permeabilities for gas and water used for the simulations were determined experimentally by Core Laboratories from three St. Peter Sandstone samples taken from the Snyder no. 2 well. The three samples have different permeability and porosity values; their connate water and residual gas saturations also differ. Data from the three samples were integrated into one drainage curve, according to the method described by Schneider (1987) (fig. 9). For the drainage curve, an irreducible water saturation of 33% was interpreted from an induction log, and an average residual gas saturation of 10.9% from the experimental data. An imbibition curve and hysteresis were modeled by the reservoir simulator.

Initial water saturation　The St. Peter Sandstone at the Hillsboro Gas Storage Field was originally an aquifer; the initial water saturation in the reservoir was 100%. The model simulated 22 years of gas storage and production from the 1973 inception of gas injection to the present.

Water Movements at Model Boundaries

Simulated reservoir models assume there is no fluid flow at the boundaries. Fluxes across the boundaries of the actual reservoir, however, may significantly influence reservoir performance. The inability to match simulated pressure values to the observed pressure values for gas- and water wells, despite adjustments in the values of porosity and water compressibility factors, shows that water movements at the boundaries significantly affected reservoir pressures. The Carter-Tracy water influx model (Carter and Tracy 1960) was used to simulate an artificial infinite aquifer outside the model boundaries. The match between simulated and observed well pressures can be fine-tuned; the size and strength of the artificial aquifer attached to each model boundary
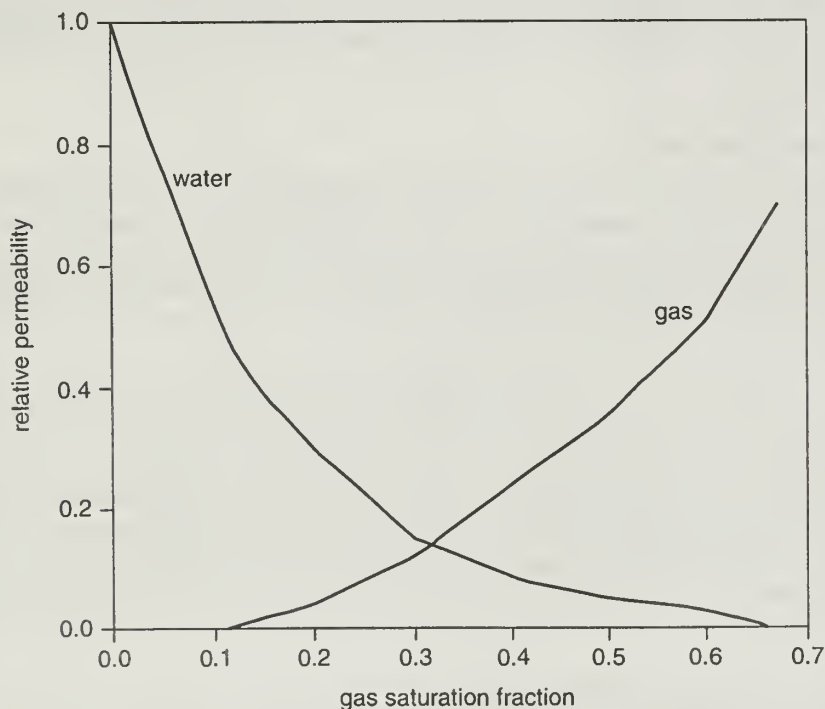

Figure 9 Gas-water relative permeability data for the St. Peter Sandstone.

are adjusted by parameter b_1 (barrels/pounds per square inch absolute [psia]), as defined by Carter and Tracy (1960):

$$b_1 = \frac{2\pi\phi c_i hr^2 s}{5.615}$$

and a dimensionless time conversion factor, t_c (1/day),

$$t_c = \frac{0.006238k}{c_t \phi \mu r^2}$$

where

ϕ = average porosity of the reservoir expressed as a fraction,

c_t = total compressibility of the fluid and rock in the aquifer (1/psia),

h = net thickness (feet) of the reservoir,

r = radius (or length for linear aquifers) (feet) to the boundary between the reservoir and the aquifer,

s = fraction of a circle completed by the boundary between the reservoir and the aquifer,

k = average permeability (millidarcies) of the reservoir, and

μ = average viscosity of water (centipoise) contained in the reservoir.

Other fluid and reservoir properties Table 3 shows values of other fluid and reservoir properties required for the model initialization. These values are fairly well known and do not require modification during the time-dependent simulations (Udegbunam and Huff 1994).

History Matches

History match runs for the period of operation between August 1973 and March 1995 were used to test the reservoir simulation model's capability to reproduce observed field performance. Data available for comparison with simulated results during part or all of this period included the total gas-in-place volumes, the bubble thickness, and the reservoir pressures at the Triutt no. 1 gas well and the four water observation wells.

The total gas inventory during this period was matched to historical values (fig. 10). Reservoir pressure matching was achieved primarily by adjusting the parameters in the Carter-Tracy artificial aquifer model. The pressure matches in the gas bubble (fig. 11) and the four water observation wells (figs. 12–15) were able to be correlated satisfactorily. Saturation matches were verified, in the absence of any produced water data, by comparing the simulated gas thicknesses to those determined from the neutron logs. The simulated gas thicknesses were within 88% of the observed values (fig. 16).

Calibration of Well Hydraulics

In this study, well hydraulics were calibrated by matching field production to a prescribed withdrawal performance: (1) withdraw up to 70% of working gas in storage

Table 3 Values of various other fluid and reservoir properties

Properties	Values
Rock compressibility, psi^{-1}	3.0×10^{-6}
Gas specific gravity (air = 1.0)	0.60
Water formation factor, reservoir BBL/STB[1]	1.01
Water specific gravity	1.0
Water viscosity, cp	1.0
Reservoir temperature, °F (°C)	85 (30)
Initial gas saturation, fraction	0.0
Datum for model initialization, feet (m)	–2595 (–791)
Initial aquifer pressure, psia (at datum)	1338

[1]Reservoir barrels/stock barrels.
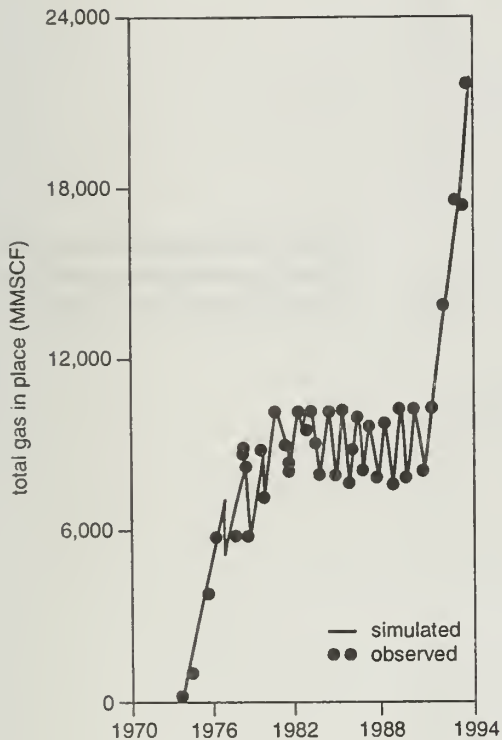
Figure 10 History match of the total Hillsboro Field gas-in-place inventory.
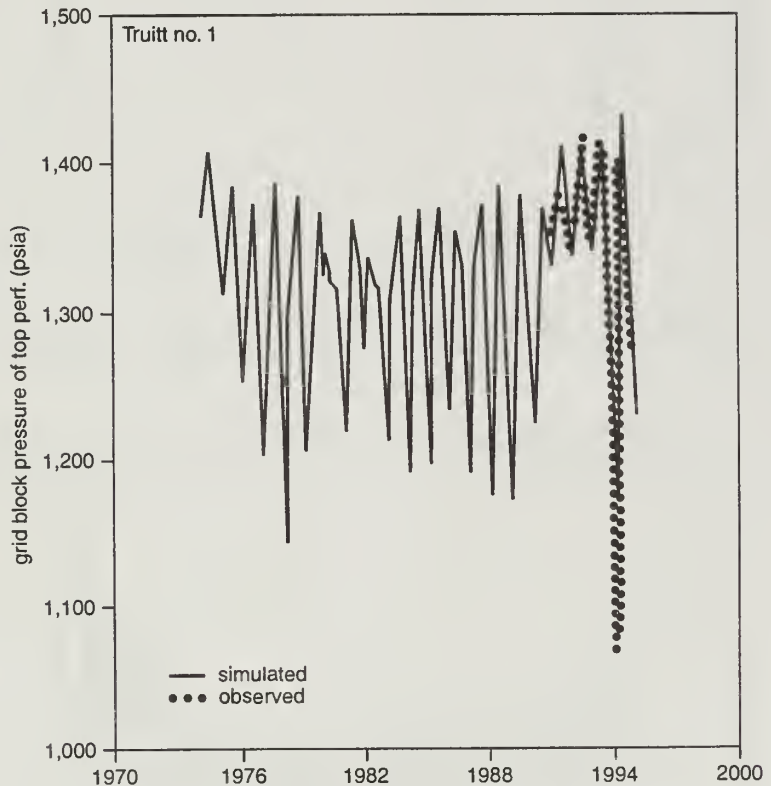
Figure 11 Simulated pressure versus observed pressure in the gas bubble at the Truitt no. 1 well.

before the peak day and (2) achieve a peak-day rate of 125 MMSCFD or more at an average surface pipeline pressure of 700 psig. This translates to a sandface bottomhole flowing pressure of about 750 psig at 2,520 feet below sea level. Field production matched these withdrawal requirements; there was no need to adjust any well parameters.

This approach was chosen in lieu of calibrating individual gas wells because combined injection/withdrawal data from station meters are more readily available than individual well data from orifice meters.

Figure 12 Simulated pressure versus observed pressure in the aquifer at the King no. 1 well.

Figure 13 Simulated pressure versus observed pressure in the aquifer at the House no. 1 well.
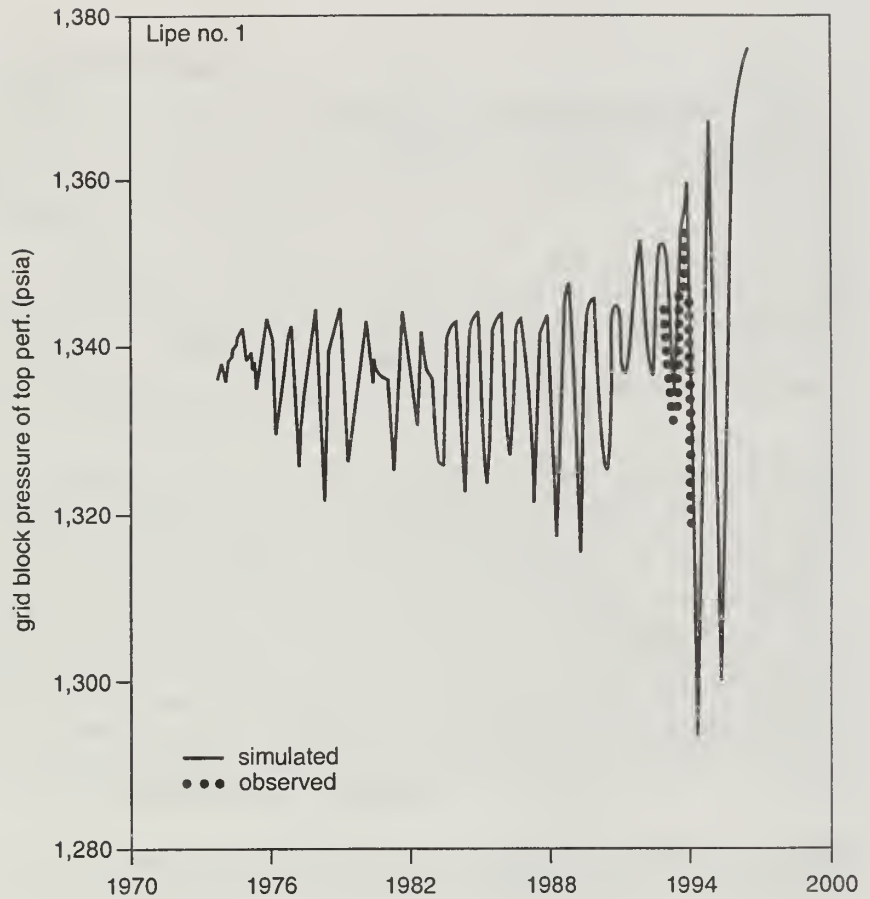
Figure 14 Simulated pressure versus observed pressure in the aquifer at the Lipe no. 1 well.

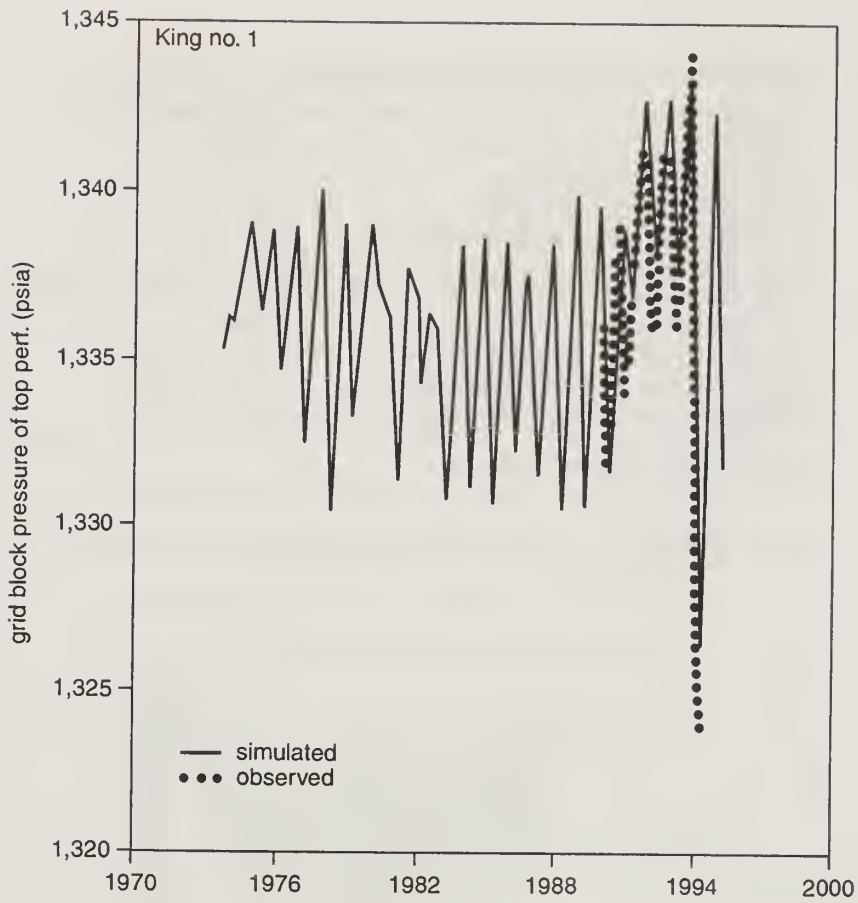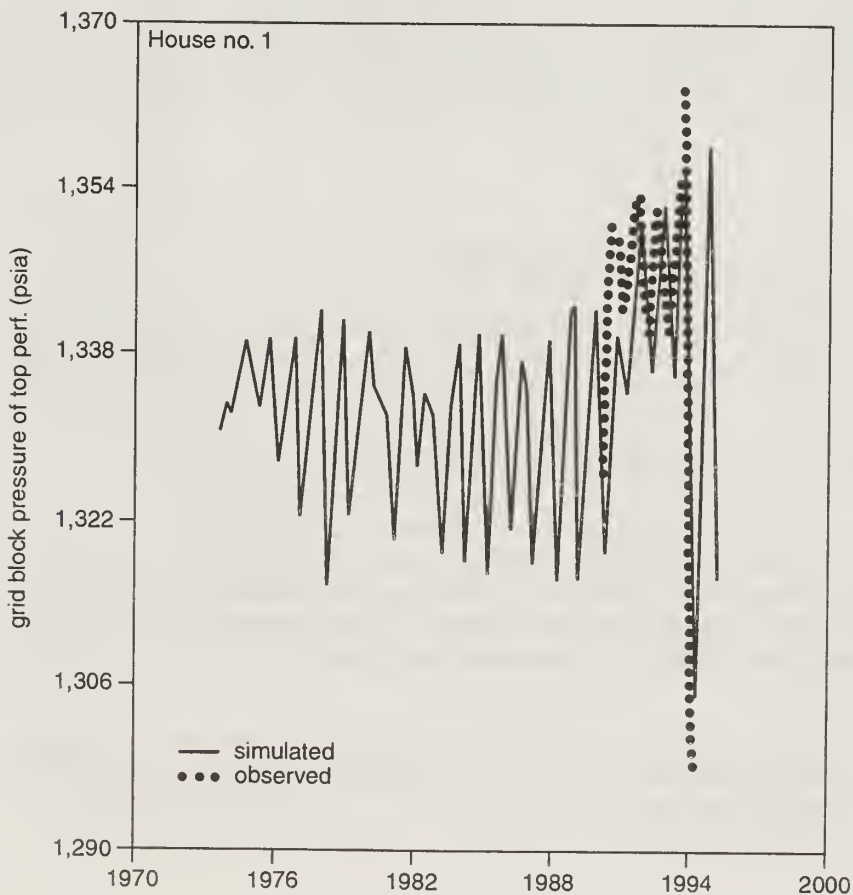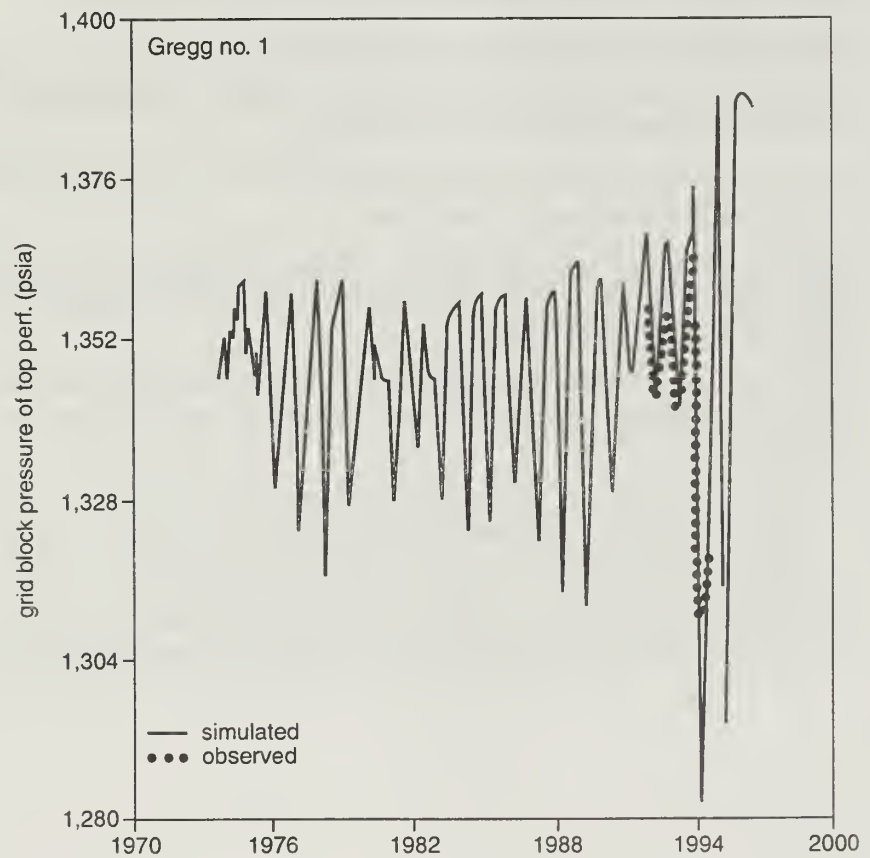**Figure 15** Simulated pressure versus observed pressure in the aquifer at the Gregg no. 1 well.
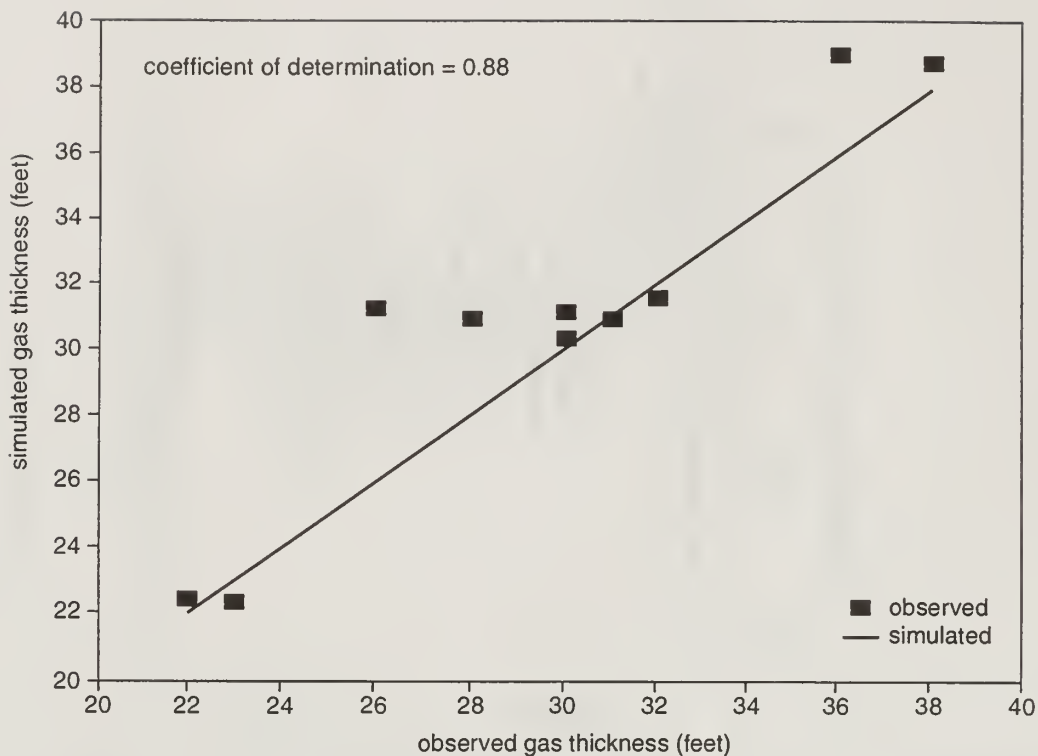
Figure 16 Simulated gas thickness versus observed gas thickness.

Investigation of the Gas Storage Field Performance

Two questions were addressed by this investigation:

1. What is the maximum simulated gas inventory that can be stored in the Hillsboro Field without gas migration at the spill points?

2. What optimum base load delivery rate will result in a maximum peak-day rate of 125 MMSCFD or more in a given year?

Investigations of future gas storage performance were simulated for the period from April 1, 1995, to March 31, 1998. Three possible strategies for gas storage development were independently investigated:

- *Base case simulation of no new development.* The maximum safe gas inventory and the optimum base load rate at the present level of development were assessed.

- *Re-completion strategy with deeper gas injection.* The effects of gas storage at greater depths, by injecting into lower layers of the sandstone, on maximum storage volume and gas deliverability were examined.

- *Additional well strategy.* The incremental gas storage volume and deliverability of new wells drilled at strategically prescribed locations were examined.

Base Case Simulations

In the base case simulations, the maximum gas-in-place volume without migration (maximum safe inventory) and the optimum base load rate were investigated at the present level of development. The simulated injection/withdrawal operations utilized all 13 active injection/withdrawal wells.

Gas-front movements   The maximum gas-in-place was determined by examining the gas/water front at different total gas-in-place volumes. Simulations (fig. 17) show that the gas-water front propagates in all lateral directions as the gas-in-place volume increases. They also suggest that the gas/water front was in the vicinity of the Gregg no. 1 observation well by the end of the 1994 injection season when the total gas-in-place volume was 21.7 BSCF.

Gas saturations at observation wells   Variations in the simulated gas saturations with the total gas-in-place at the four observation wells are shown in figure 18. These results show an increase in gas saturation at the Gregg no. 1 well from 5% when the total gas-in-place is 20.36 BSCF to 18% when the total gas-in-place is 23.8 BSCF. During the same period, gas saturation at the House no. 1 well rises from zero to about 9%, while the saturation at the Lipe no. 1 well rises from zero to about 3%. The simulated results also show that there was a gas saturation of about 5% a short distance north of the Lipe no. 1 well at a total gas-in-place of 22.6 BSCF before any gas reached the well. No gas saturation occurred in the model near or at the King no. 1 well during these simulations. Gas saturations below 11% are immobile, according to the relative permeability measurements used in this model.

Reduction of injection rates in the peripheral wells did not seem to affect gas migration trends. This reduction was achieved by halving the injection rates in the Gregg no. 2 (no. 2 in fig. 8a) Snyder no. 1 (no. 12 in fig. 8a), and Snyder no. 2 (no. 16 in fig. 8a) wells.

These results suggest that increasing the total gas-in-place beyond the present volume (21.7 BSCF) may result in significant gas migration beyond the known limits of the gas storage reservoir. Additional geological and/or geophysical studies would be needed to determine whether the gas bubble is approaching spill points beyond the observation wells that are the present limits of control.

The optimum base load volume that permits achievement of a peak-day rate of 125 MMSCFD or more (at present level of development) was examined. A gas withdrawal rate of 125 MMSCFD or more is required on the coldest day (usually in February) to supplement pipeline supplies. For planning purposes, it is necessary to know what optimum base load gas volume would still permit the required peak rate after a minimum of 70% of the working gas has been withdrawn. The model assumes that all the working gas (35% of total gas volume) is withdrawn at the end of the withdrawal season and that the local pressure drawdown between the Truitt no. 1 (no. 17 in fig. 8a) and the IP no. 1 (no. 11 in fig. 8a) wells should not exceed 100 psig to prevent sand production.

Simulated results suggest that a peak-day rate of 150 MMSCFD can be achieved with up to 70% of the working gas withdrawn (total gas volume being 22 BSCF). The peak-day rate only falls below 125 MMSCFD when 85% or more of the working gas is withdrawn prior to the peak day (fig. 19). In all the simulated cases, pressure drawdown between the Truitt no. 1 and the IP no. 1 wells remained below 15 psi.

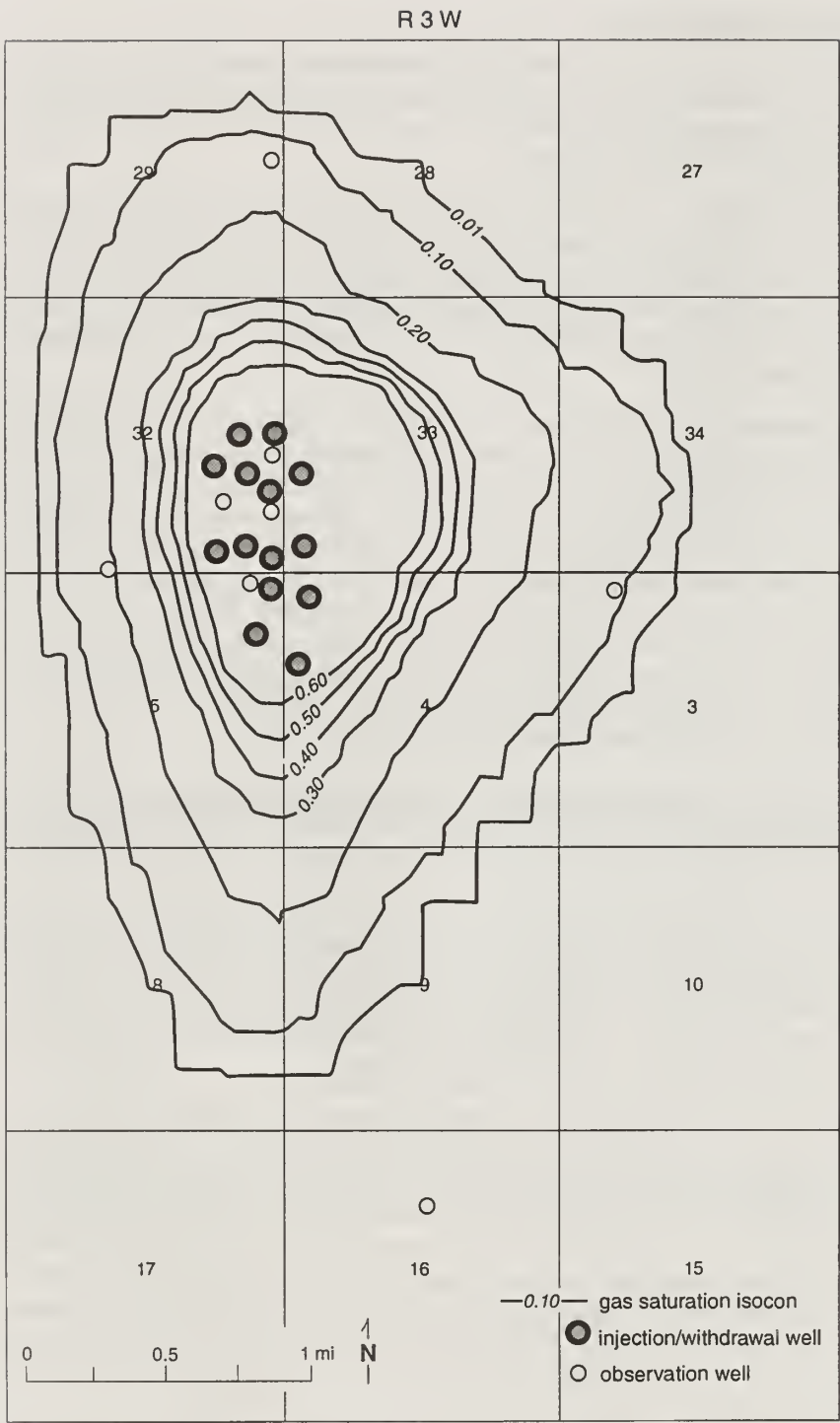**Figure 17** Gas saturation map at the end of 1994 injection season with total inventory at 21.7 BSCF. Contour interval = .10 percent except lower isocon, which is .09.
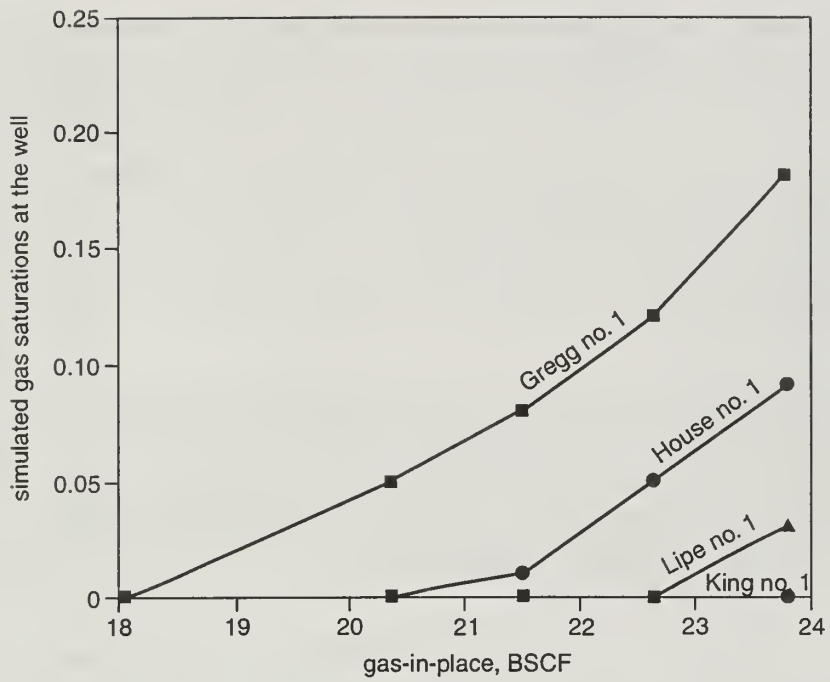
Figure 18 Gas saturations at the water observation well locations for various total gas volumes in the reservoir at the present level of field development.
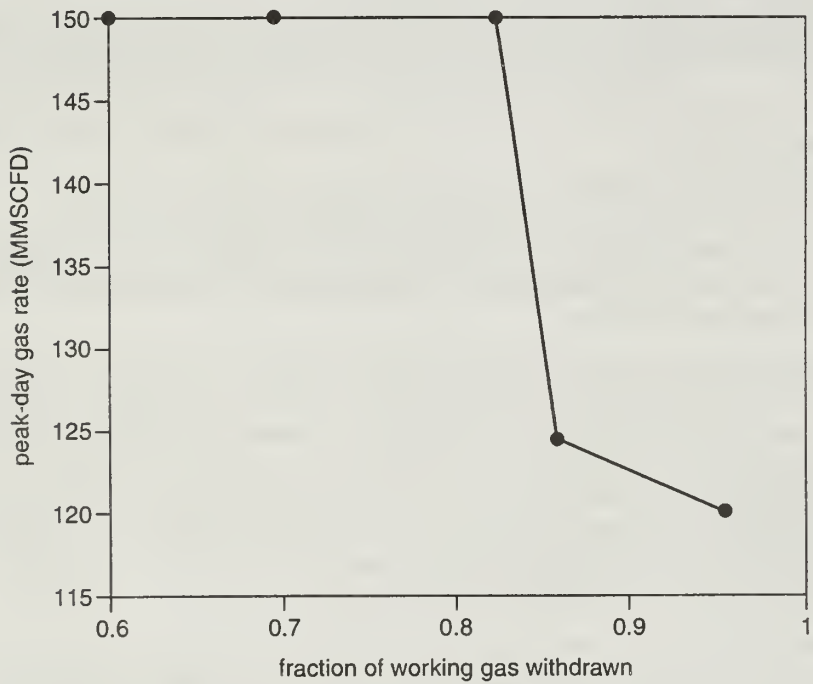

Figure 19 Field deliverability at the present level of field development.
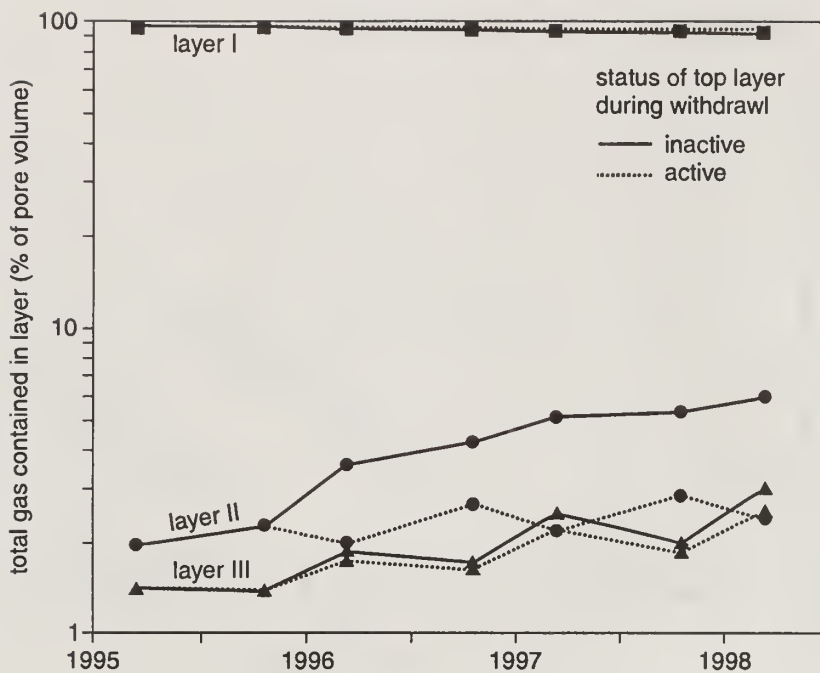
Figure 20 Simulated total gas volumes in the top three layers at different times when injection and production are only through layers 2 and 3.

Simulations of Deeper Gas Injection

Extending gas storage into lower layers at the Hillsboro Field may provide a way to increase storage and gas deliverability. The simulations address these questions:

- Is it possible to make a thicker gas bubble in the Hillsboro Field with the existing wells?

- What will be the effect of this storage strategy on gas deliverability?

In most wells, the existing well perforations occur in the upper St. Peter Sandstone at depths equivalent to the first simulation layer. In others, they correspond to the first and second simulation layers.

Simulation results prior to the beginning of the prediction runs (April 1, 1995) show that 96.6% of the gas resides in the top layer, whereas only 2% resides in the second layer, and 1.4% in the third layer (fig. 20). The presence of gas in the third layer suggests that there is gas transport between adjacent layers. Gas injection into the lower layers was increased by simulating the model perforations as sealed (inactive) in the top layer while those in the second and third layers remained open (active). In practice, this would be analogous to injecting gas into the lower depths by temporarily or indefinitely sealing off the top gas-filled layer.

The effects of this storage strategy were investigated for two gas withdrawal strategies: (1) inactive top layer (no withdrawal through the top layer and no injection) and (2) active top layer (withdrawal through top layer but no injection). During these simulations, the gas bubble grew at an incremental rate of 4 BSCF/year.

The simulations of both strategies showed that the bulk of the injected gas migrated through the lower layers to the top, inactive layer (fig. 20). The simulated total gas volume in the top layer increased from 26.6 BSCF in 1995 to more than 30 BSCF in

24

1997, regardless of whether top layer perforations were active or not during gas withdrawal. This is because there are considerable vertical transmissibilities as well as lower gas bubble pressures. Although small, the simulated total gas volumes within layers 2 and 3 continued to increase from 1995 to 1997 (fig. 20).

Consistent with the earlier results (fig. 17), gas saturations were close to the known limits of the gas storage reservoir in the top layer. Simulated injection of gas into lower depths of the reservoir did not considerably reduce gas volumes in the top layer, nor was there lateral gas expansion from the top layer within the time considered (1995 to 1998) because gas injected into the lower layers preferentially migrated to the top layer.

Gas deliverability is strongly affected by the status of the producing well perforations. The peak-day gas deliverability is very poor when the top layer is inactive (sealed), but excellent when active. It is not possible to achieve a peak-day rate of 125 MMSCFD when the top layer is inactive during withdrawal. On the other hand, it is possible to achieve a peak withdrawal of 147.7 MMSCFD, with up to 93% of the working gas withdrawn prior to the peak day, when the top layer is active during gas withdrawal (table 4).

Simulation of Effects of New Wells

The separate and collective effects of three new wells on simulated gas deliverability were examined. The wells, which are all high on the structure, are strategically consistent with the existing injection/withdrawal well pattern. One well (IP no. 5, or well 19 in fig. 8a) was placed one well spacing (660 feet) east of the IPC no. 1 well, another (IP no. 6, or well 20 in fig. 8a) was placed one well spacing west of the Morrell no. 2 well, and the last one (IP no. 7, or well 21 in fig. 8a) was placed two well spacings east of the Morrell no. 3 well. The wells were simulated one after the other and then collectively. Because injecting gas through the new wells would alter gas migration, the wells are only used for withdrawal in the model.

The following assumptions were made:

- Line pressure is 715 psig on the peak day and 1000 psig after the peak day.

- Base load withdrawn prior to peak day is 70% of working gas.

- Maximum gas inventory is maintained at 22.04 BSCF.

Table 4 Effect of the status of the top layer on the simulated gas production and the peak-day rate.

Year	Status of top layer[1]	Gas production	Peak day rate (MMSCFD on Feb. 16)
1995–96	I	66.6	100.7
	II	75.0	147.7
1996–97	I	70.0	118.0
	II	81.7	147.7
1997–98	I	70.0	119.0
	II	92.6	147.7

[1]I, inactive top layer; II, active top layer.
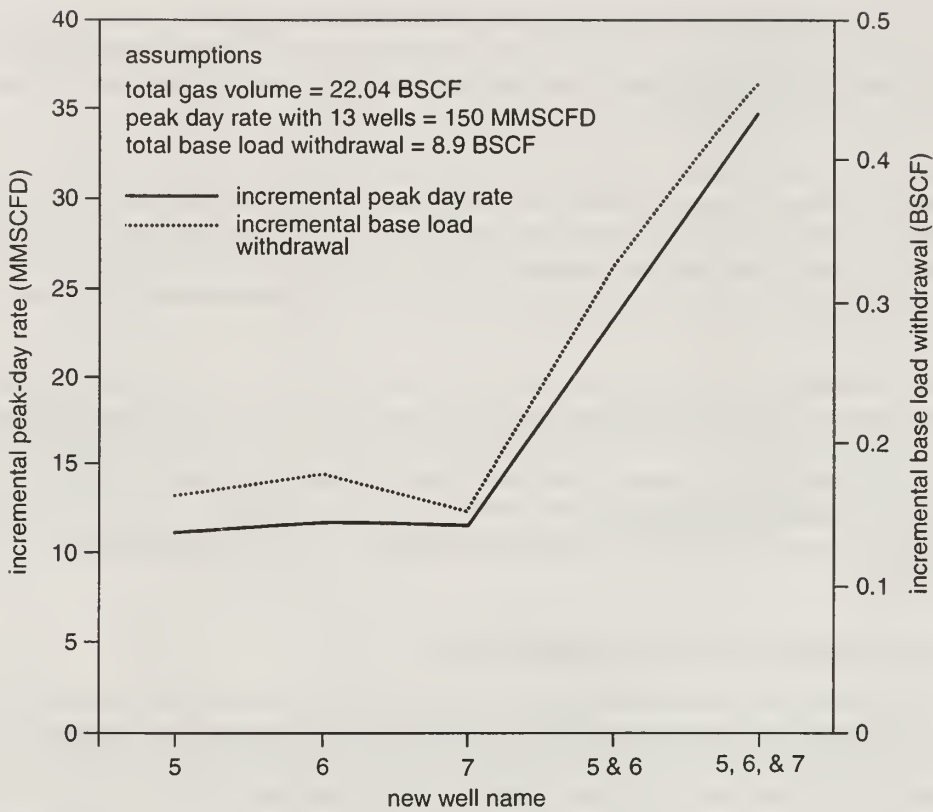
Figure 21 Individual and combined effects of three new wells on the incremental peak-day rate and the incremental base load withdrawal.

Table 5 Incremental peak-day rate and incremental volume of gas withdrawn after the addition of new wells.

	New withdrawal wells				
	no. 5	no. 6	no. 7	nos. 5 and 7	nos. 5, 6 and 7
Incremental peak dayrate over existing 13 I/W[1] wells, %	7.4	7.7	7.6	15.4	23.1
Incremental volume of gas withdrawn after addition of new wells, %	2.9	3.2	2.7	5.8	8.1

[1]Injection/withdrawal.

With the 13 existing wells, the model gives a cumulative base load delivery of 8.9 BSCF and a peak-day rate of 150 MMSCFD. The simulations (fig. 21 and table 5) show that addition of any of the wells gives incremental peak-day rate of about 11 MMSCFD and increases the total gas withdrawn by about 0.17 BSCF. Comparison of the individual well performance shows only very slight differences. The IP no. 6 well contributed the greatest incremental base load gas volume as well as the incremental peak-day rate. The addition of two or even three wells would give a proportional boost to the peak-day rate and the total base load gas withdrawal.

SUMMARY

- A 3-D reservoir flow model developed from geological and petrophysical data was used to understand and predict the performance of the Hillsboro Field gas storage reservoir. The reservoir simulation model consisted of $20 \times 28 \times 3$ grid blocks. The model layers were created on the basis of hydraulic flow units determined from the hydraulic radius concept.

- Matches between simulated results and historically observed data were satisfactory. Values matched were gas-in-place from 1973 to 1994, gas thicknesses in the gas wells at different times, and reservoir pressures at a gas well, the Truitt no. 1, and at the four water observation wells. Core permeability values were adjusted by a factor of 1.6 in the model to match values determined from well tests. No other alterations in permeability or porosity values were necessary to achieve matches between the model and historical data. Pressure matches were fine tuned by using the Carter-Tracy aquifer model to simulate an infinite aquifer and pressure support at the model boundaries.

- Performance of the gas storage reservoir under three development strategies was investigated. The strategies included (1) the base case of no new developments, (2) gas injection into lower depths, and (3) drilling of new wells.

CONCLUSIONS

- Results of the base case simulations suggest that by the end of the 1994 injection season there was gas saturation in the vicinity of the west water observation well, Gregg no. 1. According to the simulated results, increasing the total gas inventory from 21.7 BSCF to 23.8 BSCF would cause gas to migrate to the Lipe no. 1 (east observation well) and the House no. 1 (north observation well). No gas saturation occurred in the model at the south observation well (the King no. 1). A simulated peak-day delivery of 150 MMSCFD was achieved in the base case simulations with up to 80% of the working gas withdrawn prior to the peak day. The peak-day rate fell below 125 MMSCFD when 85% or more of the working gas was produced prior to the peak day.

- Simulations of gas injection and possible storage at lower depths showed that more than 96% of the total gas migrated to and is stored in the top layer, even when only the lower layers were open during gas injection. The simuated results suggest that storage enlargement through gas injection into the lower layers may not prevent gas migration. Peak-day gas deliverability was very poor when the top layer was sealed during gas withdrawal but excellent and improved when the top layer was open.

- Three strategically located new wells were simulated individually and collectively. The incremental contributions of the new wells to peak-day rate (11 MMSCFD) and to the base load withdrawal (0.17 BSCF) were nearly similar. The addition of two or three wells boosts the simulated deliverabilities proportionally.

REFERENCES

Abbaszadeh M., H. Fujii, and F. Fujimoto, 1996, Permeability prediction by hydraulic flow units: SPE Formation Evaluation Journal, December 1996, v.11, no. 4, p. 263–271.

Amaefule, J., O. Altunbay, D. Tiab, D.G. Kersy, and D.K. Keelan, 1993, Enhanced reservoir description: Using core and log data to identify hydraulic (flow) units and predict permeability in uncored intervals/wells, Paper SPE 26436. Proceedings of the1993 Annual SPE Conference and Exhibitions, Houston, Texas, October 3–6, 1993, p. 1–14.

Carter, R.D., and G.W. Tracy, 1960, An improved method for calculating water influx: Transactions of the AIME, v. 219, p. 415–417.

Dapples, E. C., 1955, General Lithofacies Relationships of St. Peter Sandstone and Simpson Group: AAPG Bulletin, v. 39, no. 4, p. 444–467.

Dott, R. H. Jr., C. W. Byers, G.W. Fielder, S. R. Stenzel, and K. E. Winfree, 1986, Aeolian to marine transition in Cambro-Ordovician Cratonic Sheet Sandstones of northern Mississippi Valley: U.S.A. Sedimentology, v. 33, p. 345–367.

Fu, R., G. Wilson, and M. Dixon, 1994, Final report: Reservoir characterization study, Hillsboro expansion project, Hillsboro Gas Storage Field, Montgomery County, Illinois. File No.: G-2085: unpublished report submitted to Illinois Power Company, September 15, 1994, OMNI Laboratories, Houston, Texas.

Land, C.S., 1968, Calculation of imbibition permeability of two-phase and three-phase flow from rock properties: SPE Journal, June 1968, p. 149–156.

Schneider, F.N., 1987, Three procedures enhance relative permeability data: Oil and Gas Journal, May 4, 1987, v. 85, no. 18, p. 45–51.

Shaw, T.H., and B.C. Schreiber,1991, Lithostratigraphy and depositional environments of the Ancell Group in central Illinois: A Middle Ordovician carbonate-siliciclastic transition, A.J. Lomando and P.M. Harris, eds., in SEPM Core Workshop no.15: Mixed carbonate-siliciclastic sequences, 1991.

Stratamodel Inc., 1993, Stratigraphic geocellular modeling, Reference manual: Stratamodel Inc., Houston, Texas, 662 p.

Udegbunam, E.O., and B.G. Huff, 1994, Geological characterization and 3D visualizations of the gas storage reservoir at Hillsboro Field, Montgomery County, Illinois, paper SPE 29158. Proceedings of the 1994 Eastern Regional Conference and Exhibition of the Society of Petroleum Engineers, Charleston, West Virginia, p. 15–30.

Udegbunam, E.O., C. Kemppainen, and J. Morgan, 1995, A reservoir model for Hillsboro Gas Storage Field management, paper SPE 30999, Proceedings of the 1995 Eastern Regional Conference and Exhibition of the Society of Petroleum Engineers, Morgantown, West Virginia, p. 163–180.

Western Atlas International, 1994, VIP Reservoir Simulator, VIP-CORE Reference Manual, Western Atlas Software: Western Atlas International, Houston, Texas. 266 p.

Wilkinson, L., 1989. SYSTAT: System for Statistics: SYSTAT, Inc., Evanston, Illinois, 822 p.